Available online at www.sciencedirect.com
ScienceDirect
Physica A 371 (2006) 781–789
PHYSICA A
www.elsevier.com/locate/physa

Synchronization of Rössler oscillators on scale-free topologies

Soon-Hyung Yook[a,b], Hildegard Meyer-Ortmanns[a,*]

[a]School of Engineering and Science, International University Bremen, P.O. Box 750561, D-28725 Bremen, Germany
[b]Department of Physics and Research Institute of Basic Sciences, Kyung Hee University, Seoul 130-701, Korea

Received 5 January 2006; received in revised form 10 April 2006
Available online 23 May 2006

Abstract

We study the synchronization of Rössler oscillators as prototypes of chaotic systems on scale-free complex networks. As it turns out, the underlying topology crucially affects the global synchronization properties. In particular, we show that the existence of loops facilitates the synchronizability of the system, whereas Rössler oscillators do not synchronize on tree-like topologies beyond a certain size. Moreover, it is not the mere number of loops that counts for synchronization but also the type of loops. By considering Cayley trees modified by additional loops in different ways, we find out that also the distribution of shortest path lengths between two oscillators plays an important role for the global synchronization.

Keywords: Networks; Complex systems; Synchronization

1. Introduction

Synchronization is a ubiquitous phenomenon in nature, ranging from flashing fireflies in the Australian forest [1], crickets chirping in unison [2] in natural systems, tremors in Parkinson's disease or epilepsy in medical applications [3], laser arrays [4], or Josephson junctions in physics [5], electrochemical oscillators in chemistry [6] and designed synchronization in robotics. Synchronization properties of limit-cycle oscillators were studied in a number of papers (for a review see Ref. [7]). In particular, recent results on the synchronization transition of a modified Kuramoto model on scale-free networks show that the details of the underlying topology such as the type of intermodular connections can crucially affect the properties of the synchronization transition [12]. Even systems which are individually chaotic like Rössler oscillators, can synchronize under certain conditions. Rössler oscillators may be regarded as prototype of chaotic systems. According to a conjecture of Calenbuhr and Mikhailov [8], the behavior of Rössler oscillators shows some universal features. For a certain class of interactions and under the influence of noise, clusters of synchronizing oscillators form above a certain threshold in the coupling strength, while for larger couplings, after an intermittent phase, the whole set of oscillators synchronizes.

Rössler oscillators were studied for different interaction schemes and on different geometries [9–11]. Usually the synchronization properties of regular networks were compared with those of scale-free or small-world

*Corresponding author. Tel.: +49 421 200 3221; fax: +49 421 200 3229.
E-mail address: h.ortmanns@iu-bremen.de (S.-H. Yook).

0378-4371/$ - see front matter
doi:10.1016/j.physa.2006.04.116

networks. The improved synchronizability of scale-free and small-world networks was usually addressed to the shorter average lengths of shortest paths. However, as it was shown in Ref. [11], it is not the average shortest path length alone that determines synchronizability, but when it goes along with stronger heterogeneity, the heterogeneity acts against synchronization. A possible explanation was provided in Ref. [10] by a comparison with a diffusive process, accounting for the very fact that "information" does not only spread along the shortest path. Our results point in the same direction that the average shortest path is not the essential criterion for synchronizability, but instead of comparing regular with scale-free and small-world topologies, we focus mainly on scale-free topologies. Scale-free networks seem to be realized in a number of natural and artificial systems like genetic or proteomic networks, the world-wide-web and the internet. Synchronization is certainly one of the important dynamical processes, running on these networks, as it is supposed to be a necessary ingredient for the efficient organization and functioning of coupled individual units, that, after all, lead to well coordinated behavior in time. Therefore, we are interested in the compatibility of scale-free topologies with synchronization, in particular for the case that the individual dynamics are chaotic. While usually the synchronization transition has been studied as a function of the coupling strength or the system size, we describe here (in addition to the usual approach) a transition to the synchronized phase as a function of the topology. In particular, we vary the topology by means of the parameter m defined in the growth algorithm of Barabási and Albert, where m denotes the number of newly attached edges in a single step [13]. As we shall see, when a "scale-free" tree (obtained for $m = 1$) becomes too large in size to allow synchronization, whatever the size of the coupling is, synchronization becomes possible beyond a critical threshold in the coupling as soon as $m > 1$. One characteristic difference of topologies with $m > 1$ as compared to $m = 1$ is certainly the contents of loops, the larger m, the more loops. The natural question then is, whether it is the mere number of loops or also a specific type of loops that facilitates synchronization? In order to answer this question we introduce loops into Cayley trees in a controlled way. As a result, we shall see that again it is not the average shortest path, but the absence of long tails in the distribution of shortest paths that matters. In other words, the essential loops are those which simultaneously provide shortcuts.

In Section 1, we introduce the model and define the order parameters that are used to distinguish the phases with and without the condensates of synchronized oscillators. In the second section we describe details of the simulations and summarize the results in the last section.

2. The model

As prototype of a chaotic system we consider N Rössler oscillators, distributed on the nodes of a scale-free network, generated with the growth algorithm of Barabási and Albert [13] (see below). Each individual oscillator at node i, $i \in \{1, \ldots, N\}$ is described by three variables x_i, y_i, z_i. These variables satisfy a set of dynamical equations that were originally proposed by Rössler [15] for describing chaotic oscillators similar to those known from the Lorenz equation [16]. Meanwhile this model is considered as one of the prototypes for chaotic behavior that easier yields synchronization than the Lorenz system. The dynamical equations are given by

$$\begin{aligned} \dot{x}_i &= -\omega y_i - z_i, \\ \dot{y} &= \omega x_i + a y_i, \\ \dot{z}_i &= b - c z_i + x_i z_i. \end{aligned} \tag{1}$$

For $\omega = 1$, $a = 0.15$, $b = 0.2$, $c = 8.5$ the system is in the chaotic state. For this choice of parameter values the attractor is chaotic and has a spiral shape. Since chaotic rotations in the phase space are nearly isochronous, such attractors, when coupled, can be relatively easily driven to the synchronized state. Among various possibilities of coupling these oscillators, we choose

$$\begin{aligned} \dot{x}_i &= -y_i - z_i, \\ \dot{y}_i &= x_i + a y_i + \varepsilon\,(\bar{y}_i - y_i), \end{aligned}$$

$$\dot{z}_i = b + (x_i - c)z_i + \varepsilon\,(\bar{x}_i\bar{z}_i - x_i z_i), \tag{2}$$

where $\bar{x}_i$, $\bar{y}_i$, $\bar{z}_i$ are averages defined as

$$\bar{x}_i = \frac{1}{k_i}\sum_{j=1}^{N} A_{ij}x_j \tag{3}$$

and accordingly for $\bar{y}_i$ and $\bar{z}_i$. The variable k_i denotes the degree of node i, A_{ij} is the adjacency matrix i.e., $A_{ij} = A_{ji} = 1$ if i and j are connected and 0, otherwise. This is the only place at which the topology of the network enters. Due to the coupling, the individual oscillators are forced to adjust their dynamics to that of their neighbors. Corrections, introduced by the coupling, can be proportional to instantaneous differences between the state variables themselves (second equation in (3)) or to differences between nonlinear functions of those variables (third equation in (3)). Later we check the dependence of the results on this very choice by introducing a linear coupling scheme, see Eq. (4). For $k_i = N - 1$ and $A_{ij} = 1$ for all $i,j \in 1,\ldots,N$ the system corresponds to a globally coupled population of Rössler oscillators as it was considered in Ref. [17]. In our description, the population is partially coupled rather than globally. It is coupled along the links of the scale-free network, therefore, the driving force towards the common synchronized state is produced by nearest-neighbors, whose number varies according to the scale-free degree-distribution. Since our averages are still node-dependent, the stability analysis of Ref. [17], derived for $\bar{x} = (1/N)\sum_{j=1}^{N} x_j$, ($\bar{y}, \bar{z}$ alike,) does not immediately apply. For this case of global coupling, in which the driving force tries to reduce the difference from the common synchronized state $(\bar{x}, \bar{y}, \bar{z})$, one expects a globally synchronized stable state for $\varepsilon = 1$, $a < 1$, so that all deviations from global averages exponentially decrease with time [17]. In our scheme the force drives to node-dependent average values over nearest neighbors whose number is neither regular nor $N - 1$, i.e., all-to-all. Nevertheless, we find a result quite similar to the all-to-all case: a global attractor to a synchronized state exists as long as $\varepsilon < 1.25$. The stability is evident on the level of numerical simulations.

In order to check how the results depend on the nonlinear terms $\propto xz$ of our coupling scheme, we also made some tests for the linear vector coupling defined according to

$$\begin{aligned}
\dot{x}_i &= -y_i - z_i + \varepsilon\,(\bar{x}_i - x_i),\\
\dot{y}_i &= x_i + a y_i + \varepsilon\,(\bar{y}_i - y_i),\\
\dot{z}_i &= b + (x_i - c)z_i + \varepsilon\,(\bar{z}_i - z_i),
\end{aligned} \tag{4}$$

where $i = 1,\ldots,N$, as it was used in Ref. [14].

2.1. Choice of order parameters

As first indicator for a partially or fully synchronized state, we measure the histogram of instantaneous pair distances $d_{ij}(t)$ between all pairs of nodes as a function of the simulation time, defined by [14]

$$d_{ij} = [(x_i - x_j)^2 + (y_i - y_j)^2 + (z_i - z_j)^2]^{1/2}, \tag{5}$$

where $i,j = 1,\ldots,N$. A fully synchronized state shows up as a sharp peak in the distribution of d_{ij}, since the pair distances between any two nodes approach zero. No synchronization or desynchronization in the opposite case lead to a broad distribution. As order parameters in the usual sense, that is quantities which vary between 0 and 1(0 for the desynchronized phase and 1 for the fully synchronized phase), we choose two order parameters r and s, as proposed in Ref. [14], defined in the following way:

$$r(t) = \frac{1}{N(N-1)}\sum_{i=1}^{N}\sum_{j=1, j\neq i}^{N} \Theta(\delta - d_{ij}(t)) \tag{6}$$

and

$$s(t) = 1 - \frac{1}{N}\sum_{i=1}^{N}\prod_{j=1, j\neq i}^{N} \Theta(d_{ij}(t) - \delta), \tag{7}$$

where $\Theta(x)$ is the Heavyside function, i.e., $\Theta(x) = 1$ if $x \geqslant 0$ and $\Theta(x) = 0$, otherwise. Due to the finite numerical accuracy one should introduce a distance that is maximally allowed between synchronized states: a radius of a tiny sphere, inside which all states are considered as synchronized. This role is played by the parameter δ; in our computations $\delta = 0.0001$ was used. For further comments on the choice see below. The order parameter $r(t)$ gives the fraction of pairs of elements (i,j) which are synchronized at time t (i.e., $d_{ij} \leqslant \delta$). This fraction is one if all possible pairs are synchronized and zero if no pair is synchronized, intermediate values $0 < r < 1$ reflect partial synchronization. The second order parameter $s(t)$ is more sensitive to partial synchronization. The second term on the r.h.s. of Eq. (7) only contributes to the fraction if node i has no other node within a distance of δ. Therefore, s is already 1 when the total number of states is a partition of synchronized pairs without synchronization between the pairs. In general we have $r < s < 1$ (as it is confirmed in the figures below) if some elements form clusters while others are still isolated. From a simultaneous measurement of r and s it is possible to obtain some information about the partial synchronization that is usually a precursor to the fully synchronized state. In general, we measured all three functions d_{ij}, r, and s as a function of the number of iterations.

3. Measurements and results

3.1. Generating the topology

For the scale-free topology we used the growth algorithm of Barabási and Albert [13], later referred to as the BA model. In each step, one node with m edges is added to the network. It is connected to m of the formerly generated nodes according to preferential attachment. In our simulations we chose m between 1 and 10. For testing the role of the loops we used the regular topology of a Cayley tree with z edges at each node, $z = 3, \ldots, 6$. The tree structure was then modified in various ways as we shall see below. We also made some runs on a small-world topology, starting from a regular ring topology with $k = 2$ neighbors and randomly adding shortcuts to each node with probability $p = 0.01$ according to the algorithm proposed by Newman and Watts [18].

3.2. Choice of parameters

For the parameters of the individual Rössler oscillators we chose $a = 0.15$, $b = 0.20$, $c = 8.5$ throughout all simulations to make sure that the individual systems are in the chaotic regime. The total number N of oscillators was varied between $10, 50, 200$ up to 500 on the scale-free topology, and $N = 190$ on the Cayley tree. The parameter m of the growth algorithm varied between 1 and 10, the coupling strength ε was out of the interval $[0.1, 1.25]$. In the numerical simulations of Eq. (2) we used the fourth order Runge–Kutta method with a typical time-step size of $\mathrm{d}t = 0.001$ (when $N = 200$). Variation of $\mathrm{d}t$ between $10^{-12} \leqslant \mathrm{d}t \leqslant 10^{-1}$ led to qualitatively the same results.

3.3. Results for $m = 1$

Fig. 1(a) displays the results for the histogram of distances for $m = 1$, $N = 200$ and the largest possible value for the coupling $\varepsilon, \varepsilon = 1.25$, above which the numerical integration becomes unstable. For smaller couplings the distribution looks qualitatively the same. The distributions are broad and do not indicate any synchronized state. Fig. 1(b) indicates a transition to a synchronized state for $m = 2$ when the coupling ε exceeds 0.3. The histogram has two narrow peaks for $\varepsilon = 0.4$ and 0.5, indicating a synchronized state for both couplings. This result is further supported by the corresponding results in measurements of r and s as shown in Fig. 2(a) and (b), respectively, r stays zero for $m = 1$, while s increases from $\varepsilon = 0.1$ on, indicating partial synchronization. The value of $N = 200$ seems to represent the large-N limit, for the considered range of ε and m, since we obtained the same result for r and s for $N = 300, 400, 500$. On the other hand, for smaller systems, $N < 20$, we do see a fully synchronized state when the coupling ε exceeds a critical threshold. As value for δ in Eqs. (6) and (7) that accounts for the finite numerical accuracy, we choose $\delta = 0.0001$. For smaller values we observe large variations in the long-time behavior of r and s. On the other side, it is obvious that for δ too

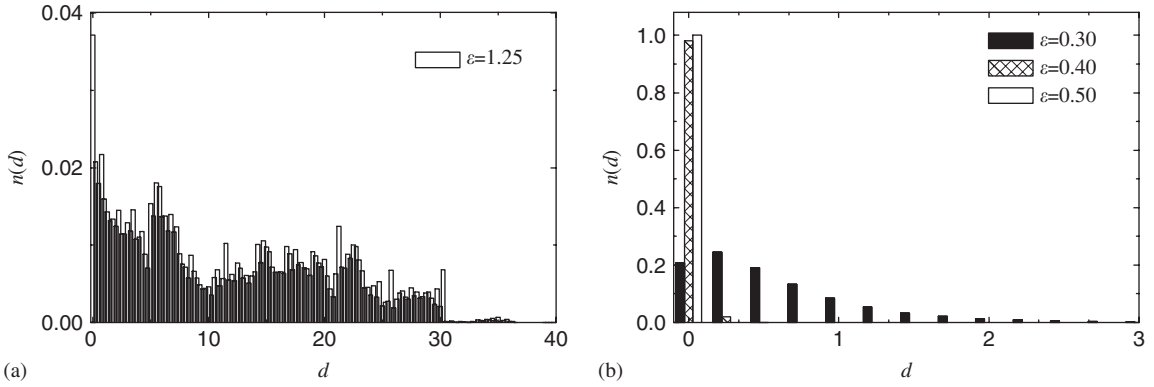

Fig. 1. Histogram of all pair distances between oscillators on a BA network with (a) $m = 1$, (b) $m = 2$, for $N = 200$ and various couplings ε, that is $n(d)$ denotes the number of pairs with distance d, normalized over the total number of pairs of the network.

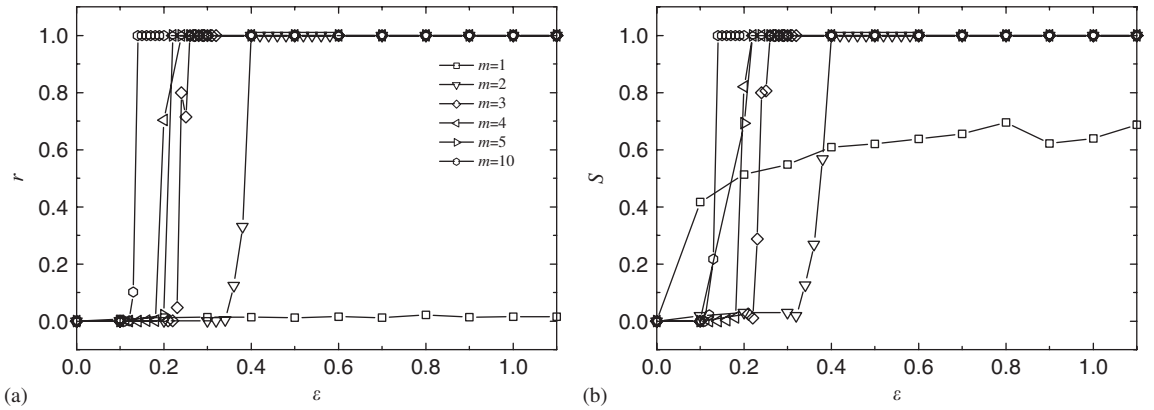

Fig. 2. Order parameters (a) r and (b) s as a function of the coupling strength ε for different values of m, $N = 200$.

large, the values of r and s are stable over time, but the larger δ, the more oscillators appear as synchronized due to the too coarse resolution. The parameters loose their sensitivity to synchronization, so that the number of synchronized oscillators gets δ-dependent, until the whole system appears as synchronized. Here $\delta = 0.1$ turned out to be an upper bound, so that $0.0001 < \delta < 0.1$ provides a window that is small enough to distinguish between synchronized and desynchronized states and large enough to make r and s insensitive to numerical fluctuations. There we find a plateau for the values of r and s, that is, the features of synchronization become independent of the size of δ.

3.4. Results for m larger than one but still integer

If we keep the number N of oscillators fixed to 200, we observe for $m > 1$ a fully synchronized state above a critical threshold in the coupling ε; this threshold is the larger the smaller m, again $r < s$ in general, as seen from Figs. 2(a) and (b).

3.5. Results for intermediate non-integer m

One of the main differences between the Barabási–Albert networks with parameter $m = 1$ and $m > 1$ is the tree-like structure for $m = 1$ and the existence of loops for $m > 1$. In order to check whether it is only the loops that facilitate synchronization and how many loops are needed, we generalized the growth algorithm to

non-integer values of m in the following way. We introduce an additional probability p_m for a new node to have $m = 1$ edges and probability $(1 - p_m)$ for having $m = 2$ edges attached to the nodes of the network when it is introduced during the growth process. The distribution of pair distances of oscillators for $1 < \langle m \rangle < 2$ is displayed in Fig. 3. From the pronounced peak in the distribution $n(d)$ for $\langle m \rangle = 1.4$ and the broader distribution for $\langle m \rangle = 1.35$ we conclude that (for the given parameters $\varepsilon = 0.9$, $N = 200$) the transition occurs between $\langle m \rangle = 1.35$ and $\langle m \rangle = 1.4$. For given N and ε we therefore observe a transition to a fully synchronized state as a function of "topology", parameterized via the parameter m. Fig. 4(a) shows that the position of the transition, now in m rather than in ε, depends on the coupling strength for fixed N. The smaller ε, the larger m_c. An interesting feature is seen in Fig. 4(b), where s is plotted as a function of m. For $\varepsilon = 0.3$ and $m = 1$, the finite value of s indicates some partial synchronization, s then drops to zero at $m = 2$ and increases to 1 for $m = 3$. As we have argued above, $s = 1$ does not necessarily imply full synchronization, but some partial one, at least. It should be noticed that the behavior of s is non-monotonic as a function of m. A similar non-monotonic behavior of s as function of time was observed in Ref. [8] for Rössler oscillators, for which a partial synchronization was followed by desynchronization, before the full synchronization set in. Obviously, in both cases there is not a "continuous" route to synchronization in the sense that a desynchronized state is followed

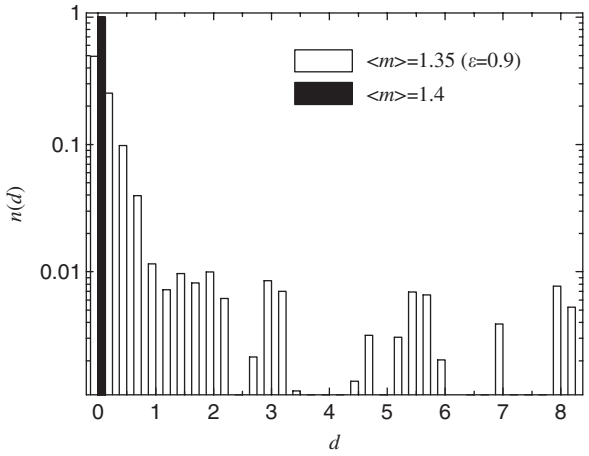

Fig. 3. Histogram of pair distances on a BA model with $1 < \langle m \rangle < 2$ with $N = 200$ and $\varepsilon = 0.9$. The diagram indicates synchronization for $\langle m \rangle = 1.4$ and no synchronization for $\langle m \rangle = 1.35$.

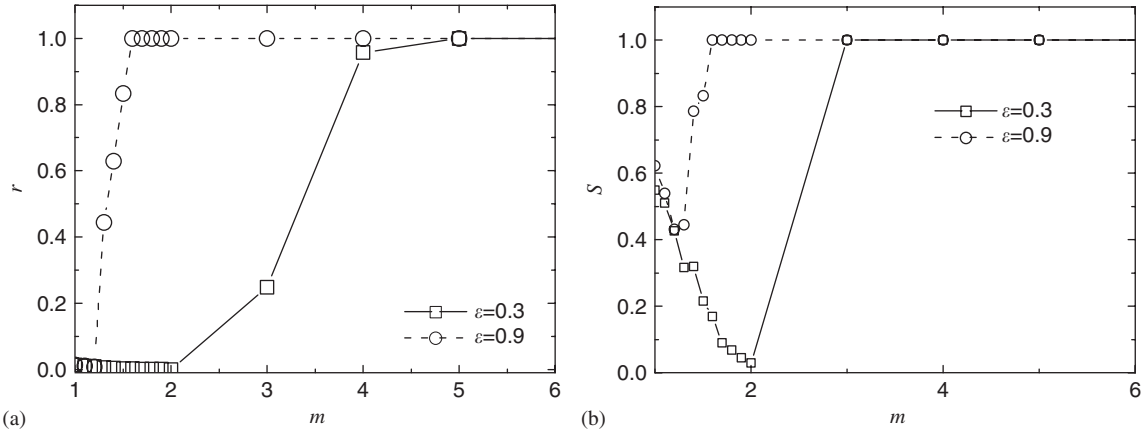

Fig. 4. Order parameters r (a) and s (b) as function of the parameter m that is used to distinguish different topologies, for two values of the coupling strength.

first by a partially synchronized and next by a fully synchronized state. With m, the number of loops increases in the Barabási–Albert network, but as we shall see in the following section, it is not the mere number of loops that determines the features of synchronization, so that we finally do not have a detailed "microscopic" understanding of the non-monotonic behavior as function of m.

3.6. Rössler oscillators on a Cayley tree

From the former results we conclude that a certain number of loops facilitates synchronization on scale-free networks, the larger m, the more loops [19], the smaller the coupling strength needed for synchronization. In order to check whether it is the mere number of loops that facilitates synchronization or also the type of loops, we studied N Rössler oscillators on a Cayley tree whose regular structure is modified in a controlled way. In version (a) we add edges with probability p_a to connect pairs of nodes with mutual distance 2. In this way, we

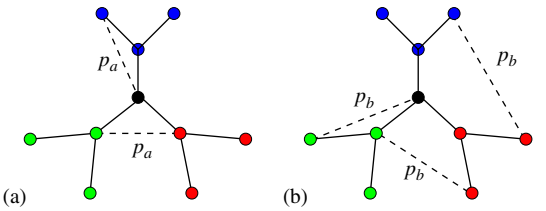

Fig. 5. Cayley tree for $z = 3$ and additional interconnections (dashed lines) attached according to the two rules (a) and (b), as described in the text.

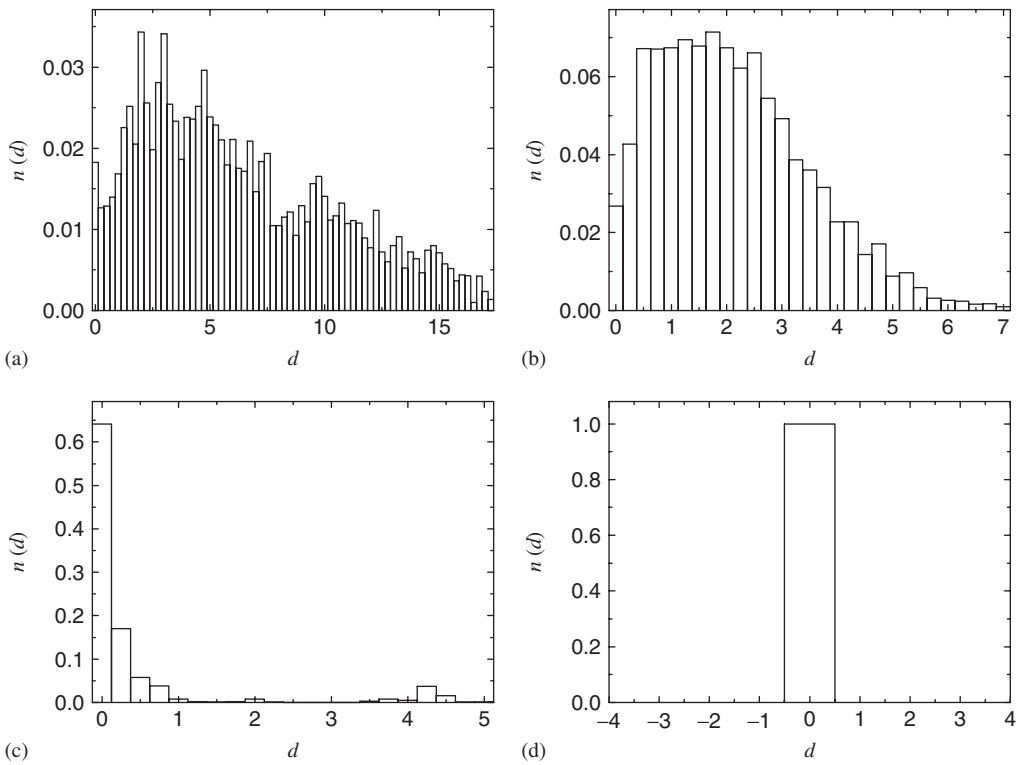

Fig. 6. Histogram of all pair distances between oscillators on Cayley trees with shortcuts generated according to rule (b). The probability of connecting any randomly chosen pair is (a) $p = 0.0005$, (b) $p = 0.001$, (c) $p = 0.005$, and (d) $p = 0.006$. The critical probability $p_c \simeq 0.006$ for the synchronization transition is almost the same as that of the small-world transition in Ref. [20]. In all cases we chose $N = 200$ and $\varepsilon = 1.0$.

introduce a certain number of triangles at random locations as typical local loops, see Fig. 5(a). In version (b) we add edges between pairs of nodes (with arbitrary mutual distance), randomly selected with probability p_b (Fig. 5(b)). The result of additional edges according to (a) is no improvement of synchronization as long as $p_a < 0.99$, as it is seen from histograms of pair distances $n(d)$, qualitatively similarly looking to those of Figs. 6(a) and (b), not displayed here. In case of edges added according to (b) we have varied the probability p_b between 0.0005 and 0.99. Already for $p_b = 0.006$ this leads to a small-world network á la Newman and Watts [18], showing synchronization in the histogram of $n(d)$, (see Fig. 6(d)). The critical probability below which there is no synchronization is given by $p_c \simeq 0.006$. Along with the histograms of $n(d)$ we have measured the distributions of shortest path lengths in the various loop-modified trees, see Fig. 7. Figs. 7(a) and (b) show asymmetric broad and non-Poissonian distributions, corresponding to phases of desynchronization, as it is obvious from Figs. 6(a) and (b). The shortest path distributions become Poissonian-like and show the absence of long tails when the system reaches synchronization in Figs. 6(c) and (d). Qualitatively, the same result we find for a synchronized Barabási–Albert network for $m = 2$ (not shown here). It is interesting to notice that it is not the average shortest path length that is responsible for synchronization. On a Cayley-tree this is easily checked by keeping the total number of nodes almost constant, but varying the coordination number z. In this way the diameter of the Cayley-tree is reduced, but independently of the value of z, synchronization is only possible if the network contains a sufficient number of shortcuts. Without shortcuts, no synchronization phase is found however small the average shortest path length is.

Long branches of trees support independent oscillatory dynamics. From the above results, we find numerical evidence that neither the mere existence of loops nor the existence of a short average-path length alone are sufficient to guarantee synchronization.

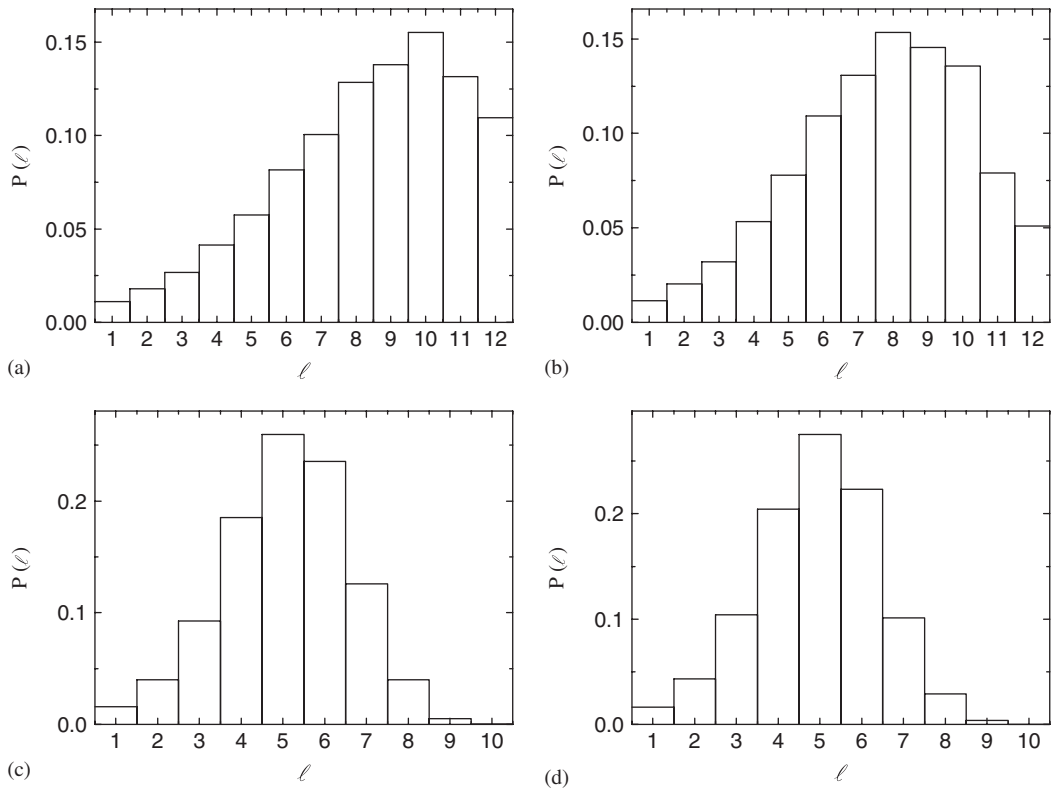

Fig. 7. Histograms $P(\ell)$ of shortest paths of length ℓ for networks with $N = 200$ Rössler oscillators on modified Cayley-trees according to (b). (a) $p = 0.0005$, (b) $p = 0.001$, (c) $p = 0.005$, and (d) $p = 0.006$. (a) and (b) show non-Poissonian distributions and correspond to desynchronization, (c) and (d) are Poissonian-like and go along with synchronization as it is obvious from Fig. 6.

4. Summary and conclusions

We studied an ensemble of Rössler oscillators on scale-free networks constructed by the Barabási–Albert growth algorithm. In contrast to the usual investigations we studied the transition from the desynchronized or partially synchronized state to the fully synchronized state as a function of the network topology, parameterized by m, the number of newly attached edges in the growth algorithm. For the tree topology ($m = 1$) and given coupling strength ε, there is a fully synchronized state below some critical size N that disappears for larger N. This result is similar to synchronization of Kuramoto oscillators on Cayley trees which is possible for small enough size N and coordination number z [21]. Above a certain number of nodes, the tree of Rössler oscillators can no longer be synchronized, however large the coupling strength is. It is then the parameter m that introduces loops and shortcuts into the tree, and along with this allows full synchronization, when m exceeds a certain value that depends on N and ε. Vice versa, the threshold in ε depends on N and m. Small N, large ε (chosen out of the stability regime) and large m favor synchronization. These qualitative results are not specific for our choice of nonlinear couplings between the Rössler oscillators, but also hold for the vector coupling scheme of Eq. (4). Moreover, numerical simulations of Rössler oscillators on Cayley trees with randomly introduced small and large loops suggest that it is not only the mere number of loops that favors synchronization, but it is also a sufficient number of loops that provide real shortcuts in the system.

Acknowledgments

This project is partly supported by the Kyung Hee University Research Fund in 2005''(KHU-20051035). One of us (H.M.-O.) would like to thank Michael Zaks for useful discussions.

References

[1] J. Buck, Nature 211 (1966) 562.
[2] T.J. Walker, Science 166 (1969) 891.
[3] R.D. Traub, R. Miles, R.K.S. Wong, Science 243 (1989) 1319.
[4] G. Kozyreff, A.G. Vladimirov, P. Mandel, Phys. Rev. Lett. 85 (2000) 3809;
A.G. Vladimirov, G. Kozyreff, P. Mandel, Eur. Lett. 61 (2003) 613619.
[5] K. Wiesenfeld, P. Colet, S.H. Strogatz, Phys. Rev. Lett. 76 (1996) 404.
[6] W. Wang, I.Z. Kiss, J.L. Hudson, Chaos 10 (2000) 248.
[7] J.A. Acebrón, L.L. Bonilla, C.J. Pérez-Vicente, F. Ritort, R. Spigler, Rev. Mod. Phys. 77 (2005) 137.
[8] A.S. Mikhailov, V. Calenbuhr, From Cells to Societies: Models of Complex Coherent Action, Springer, Berlin, 2002, pp. 169, 194.
[9] M.G. Rosenblum, A.S. Pikovsky, J. Kurths, Phys. Rev. Lett. 76 (1996) 1804;
G.V. Osipov, A.S. Pikovsky, M.G. Rosenblum, J. Kurths, Phys. Rev. E 55 (1997) 2353;
Z. Zheng, G. Hu, B. Hu, Phys. Rev. E 62 (2000) 7501.
[10] A.E. Motter, C. Zhou, J. Kurths, Phys. Rev. E 71 (2005) 016116.
[11] T. Nishikawa, A.E. Motter, Y.-C. Lai, F.C. Hoppensteadt, Phys. Rev. Lett. 91 (2003) 014101;
F.M. Atay, T. Biyikoglu, Phys. Rev. E 72 (2005) 016217.
[12] E. Oh, K. Rho, H. Hong, B. Kahng, Phys. Rev. E 72 (2005) 047101.
[13] R. Albert, A.-L. Barabási, Rev. Mod. Phys. 74 (2002) 48.
[14] D.H. Zanette, A.S. Mikhailov, Phys. Rev. E 62 (2000) R7571.
[15] O.E. Rössler, Phys. Lett. 57 (1976) 397.
[16] E.N. Lorenz, J. Atmos. Sci. 20 (1963) 130.
[17] D.H. Zanette, A.S. Mikhailov, Phys. Rev. E 57 (1998) 276.
[18] M.E.J. Newman, D.J. Watts, Phys. Rev. E 60 (1999) 7332.
[19] G. Bianconi, A. Capocci, Phys. Rev. Lett. 90 (2003) 078701.
[20] D.J. Watts, S.H. Strogatz, Nature 393 (1998) 440.
[21] F. Radicchi, H. Meyer-Ortmanns, Phys. Rev E 73 (2006) 36218.